Immune Netw. 2022 Dec;22(6):e50
https://doi.org/10.4110/in.2022.22.e50
pISSN 1598-2629·eISSN 2092-6685

IMMUNE NETWORK

Original Article

Check for updates

Low-Level Expression of CD138 Marks Naturally Arising Anergic B Cells

Sujin Lee †, **Jeong In Yang** †, **Joo Hee Lee**, **Hyun Woo Lee**, **Tae Jin Kim** *

Department of Immunology, Sungkyunkwan University School of Medicine, Suwon 16419, Korea

OPEN ACCESS

Received: Aug 30, 2022
Revised: Oct 7, 2022
Accepted: Oct 14, 2022
Published online: Oct 24, 2022

***Correspondence to**
Tae Jin Kim
Department of Immunology, Sungkyunkwan University School of Medicine, 2066 Seobu-ro, Jangan-gu, Suwon 16419, Korea.
Email: tjkim@skku.edu

†Sujin Lee and Jeong In Yang contributed equally to this work.

ORCID iDs
Sujin Lee
https://orcid.org/0000-0001-6314-5854
Jeong In Yang
https://orcid.org/0000-0002-1951-0196
Hyun Woo Lee
https://orcid.org/0000-0002-9610-8643
Tae Jin Kim
https://orcid.org/0000-0001-9802-0568

Conflicts of Interest
The authors declare no potential conflicts of interest.

Abbreviations
BCR, B cell receptor; CDR, complementarity determining region; FO, follicular; T, transitional; HEL, hen egg lysozyme; WT,

ABSTRACT

Autoreactive B cells are not entirely deleted, but some remain as immunocompetent or anergic B cells. Although the persistence of autoreactive B cells as anergic cells has been shown in transgenic mouse models with the expression of B cell receptor (BCR) reactive to engineered self-antigen, the characterization of naturally occurring anergic B cells is important to identify them and understand their contribution to immune regulation or autoimmune diseases. We report here that a low-level expression of CD138 in the splenic B cells marks naturally arising anergic B cells, not plasma cells. The $CD138^{int}$ B cells consisted of $IgM^{low}IgD^{high}$ follicular (FO) B cells and transitional 3 B cells in homeostatic conditions. The $CD138^{int}$ FO B cells showed an anergic gene expression profile shared with that of monoclonal anergic B cells expressing engineered BCRs and the gene expression profile was different from those of plasma cells, age-associated B cells, or germinal center B cells. The anergic state of the $CD138^{int}$ FO B cells was confirmed by attenuated Ca^{2+} response and failure to upregulate CD69 upon BCR engagement with anti-IgM, anti-IgD, anti-Igκ, or anti-IgG. The BCR repertoire of the $CD138^{int}$ FO B cells was distinct from that of the $CD138^{-}$ FO B cells and included some class-switched B cells with low-level somatic mutations. These findings demonstrate the presence of polyclonal anergic B cells in the normal mice that are characterized by low-level expression of CD138, IgM downregulation, reduced Ca^{2+} and CD69 responses upon BCR engagement, and distinct BCR repertoire.

Keywords: Clonal anergy; Syndecan-1; Follicular B cell; Transitional B cell; B cell receptor repertoire

INTRODUCTION

Although many autoreactive B cells are deleted to avoid the generation of autoreactive Abs, the proportion of autoreactive B cells in the periphery is considerably high. However, in most individuals, they do not cause autoimmune diseases as they are controlled by peripheral regulatory mechanisms (1-5). Removal or inactivation of autoreactive B cells depends on several mechanisms, including clonal deletion, receptor editing, anergy induction, and follicular (FO) exclusion (6-8). The phenomenon of B cell tolerance to self-Ags has been well demonstrated by many studies using high-affinity B cell receptor (BCR)-transgenic mice expressing engineered autoantigens (9,10). Interestingly, the presence of high-affinity Ags can neither delete nor anergize the autoreactive B cells completely, suggesting that

IMMUNE NETWORK

wild-type; FACS, fluorescence-activated cell sorting; DEG, differentially expressed gene; FC, fold change; qRT-PCR, quantitative RT-PCR; GSEA, gene set enrichment analysis; LAS, Life is Art of Science; KBSI, Korea Basic Science Institute; JSD, Jenson-Shannon divergence; MH, Morisita-Horn.

Author Contributions

Conceptualization: Lee S, Yang JI, Lee JH, Kim TJ; Data curation: Lee SJ, Yang JI; Formal analysis: Lee HW; Validation: Lee S, Yang JI, Lee JH; Writing–original draft: Lee S, Kim TJ; Writing - review & editing: Lee S, Yang JI, Lee JH, Lee HW, Kim TJ.

immunocompetent autoreactive B cells may develop normally (5). Furthermore, these studies cannot reflect the selection of wild-type (WT) polyclonal B cells that express randomly rearranged BCRs with low affinities to self-Ags.

Immature B cells, including autoreactive B cells, emigrate to the spleen as transitional B cells and positive and negative selection of transitional B cells shape the mature B cell repertoire based on BCR signaling (11). The majority of peripheral B cells appear to have experienced antigenic encounters via BCRs during development, according to previous studies that reported the upregulated Nur77 expression in peripheral B-cell populations (12,13). Most mature B cells express Nur77, suggesting that most B cells have encountered BCR-specific self-Ags during peripheral development. The BCR engagement with self-Ags may trigger B cell activation to a continuous level so that some B cells induce Nur77 expression, some B cells do not, and some B cells generate strong anergy-inducing signals in addition to Nur77 expression. Not only the strength but also the chronicity of BCR-mediated signaling is critical for the induction of B cell anergy (14,15).

The phenotyping and identification of polyclonal anergic B cells are important to investigate the contribution of anergic B cells to the pathogenesis of autoimmune disease. The downregulation of IgM and upregulation of IgD are a phenotype of anergic B cells and have been observed in B cells from BCR-transgenic and WT mice (16,17). Human blood anergic B cells also show an $IgM^{-}IgD^{+}$ phenotype with autoreactive BCRs (18). However, the levels of IgM and IgD are variable and continuous in FO B cells, and therefore, it is difficult to discriminate between immunocompetent and anergic FO B cells. In this study, we evaluated the usefulness of CD138 in the identification of polyclonal anergic B cells. Although CD138 is used as a marker of plasma cells, a low-level expression of CD138 has been observed in precursor and mature B cells (19,20). Furthermore, a low-level expression of CD138 was noted in anergic B cells that expressed anti-hen egg lysozyme (anti-HEL) BCRs in HEL-expressing mice (16) and diabetogenic anti-insulin B cells (21). We also observed previously that splenic $CD138^{int}$ B cells express a lower level of IgM and a higher level of IgD than splenic $CD138^{-}$ B cells (22). Here, we analyze splenic $CD138^{int}$ B cells in detail and demonstrate that $CD138^{int}$ B cells are anergic B cells belonging to transitional 3 (T3) or FO B cells.

MATERIALS AND METHODS

Mice

C57BL/6 WT and C57BL/6-Tg(IghelMD4)4Ccg/J mice were purchased from Orient Bio (Seongnam, Korea) and the Jackson Laboratory (Bar Harbor, ME, USA), respectively, and maintained in the Laboratory Animal Research Center of Sungkyunkwan University. C57BL/6-Tg(IghelMD4)4Ccg/J mice have a transgene named MD4 for IgM and IgD anti-HEL, which cannot switch to other isotypes (23). All procedures were performed in a pathogen-free facility according to institutional guidelines. This study was approved by the Institutional Animal Care and Use Committee of Sungkyunkwan University School of Medicine.

Cell preparation, flow cytometric analysis, and cell sorting

Single-cell suspensions obtained from 8–12-week-old C57BL/6 WT mice were obtained by mechanical disruption and passage through a nylon membrane. After lysis of red blood cells and washing, purified cells were stained on ice for 30 min with combinations of fluorochrome-conjugated Abs in fluorescence-activated cell sorting (FACS) buffer (5%

newborn bovine calf serum and 0.05% sodium azide in phosphate-buffered saline [PBS]). Fluorochrome-labeled monoclonal Abs against following Ags were used: CD138 (281-2), IgM^b (AF6-78), CD19 (1D3), B220 (RA3-6B2), and Sca-1 (E13-161.7) from BioLegend (San Diego, CA, USA); CD21/35 (7E9) from BD Biosciences (San Jose, CA, USA); and B220 (RA3-6B2), CD23 (B3B4), CD93 (AA4.1), IgM (II/41), and IgD (11-26c) from eBioscience (San Diego, CA, USA). Fluorescence minus one control was used to confirm the expression levels of cell surface proteins. After washing with FACS buffer, electronic data were acquired from stained cells using BD FACSCanto II (BD Biosciences) at the BIORP of the Korea Basic Science Institute (KBSI), and data analysis was performed using FlowJo software (BD Biosciences).

FACS Aria III instrument (BD Biosciences) at the BIORP of the KBSI was used to purify B220$^+$CD138^{int} and B220$^+$CD138$^-$ B cells from total splenic cells. CD138^{int} and CD138$^-$ FO B cells were sorted after staining with Abs against CD138, B220, CD23, and CD21. The purity of sorted cells was >95% (viability >85%). Viable cells were identified as Fixable Viability Dye eFluor780 (eBioscience) negative.

In vivo stimulation

For *in vivo* HEL antigenic stimulation, anti-HEL MD4 mice were injected i.p. with 100 μg of HEL (Sigma-Aldrich, St Louis, MO, USA) in PBS, and splenocytes were harvested 4, 16, 24, and 72 h later and stained with combinations of Abs, including anti-CD138 Ab.

Calcium assays

Total splenic B cells were obtained from C57BL/6 WT mice by a magnetic-associated cell sorting (MACS, eBioscience) using a MagniSort Mouse B cell Enrichment Kit (Invitrogen, Carlsbad, CA, USA) and stained with anti-B220, CD23, CD21, CD138, and 7AAD in FACS buffer on ice. Cells were washed twice with PBS and loaded with 5 μM Fluo-4 AM (Invitrogen), a calcium-sensitive dye, in Hank's balanced salt solution (HBSS; Gibco, Grand Island, NY, USA) containing 1 μM calcium and 1 μM magnesium at 37°C for 30 min. After staining, cells were washed, resuspended, and incubated in HBSS at 37°C for 10 min. After dye-loaded cells were placed on a flow cytometer, the basal intracellular calcium levels of gated B cell populations were monitored for 45 s. Then, cells were stimulated with F(ab′)$_2$ goat anti-mouse IgM, anti-mouse IgG (H+L), anti-mouse Igκ (Jackson ImmunoResearch, West Grove, PA, USA), goat anti-mouse IgD (MD Bioproducts, Zurich, Switzerland), or ionomycin (Sigma-Aldrich) in the presence of exogenous calcium in the medium. Calcium flux was assessed by fluorescence intensity for 5 min after the stimuli. Kinetic curves for each calcium response were generated using FlowJo software (BD Biosciences).

Quantitative RT-PCR (qRT-PCR)

Total cellular RNA was extracted from purified splenic B cells in C57BL/6 WT mice using a RNeasy Mini Kit (Qiagen, Valencia, CA, USA) and reverse-transcribed to cDNA using a PrimeScript™ 1st strand cDNA Synthesis Kit (Takara Bio, Siga, Japan). The qRT-PCR analysis was carried out using a QuantStudio 6 Flex Real-Time PCR System (Life Technologies, Frederick, MD, USA). TaqMan gene expression analysis was conducted with probes purchased from Applied Biosystems (Palo Alto, CA, USA). Purchased primers were for Syndecan 1 (Mm00448918_m1), Pcp4 (Mm00500973_m1), Sox4 (Mm00486320_s1), Ndrg1 (Mm07295892_m1), Rgl1 (Mm00444088_m1), and GAPDH (Mm99999915_g1). The GAPDH expression was used as the internal control.

Bulk RNA sequencing and data analysis

Bulk RNA sequencing of CD138^{int} and CD138^{-} FO B cells obtained from C57BL/6 WT mice was performed at the Life is Art of Science (LAS) Laboratory (Gimpo, Korea). Total RNA was extracted using TRIzol® RNA isolation reagents (Life Technologies, Foster City, CA, USA). Isolated total RNA was processed to prepare the mRNA sequencing library using the Illumina TruSeq Stranded Preparation Kit (Illumina, Inc., San Diego, CA, USA) according to the manufacturer's instructions. All libraries were quantified by qPCR using the CFX96 Real-Time System (Bio-Rad). High-throughput sequencing was performed on the NextSeq500 Sequencer (Illumina, Inc.) with 150-bp paired-end reads. Reads were aligned to the mouse reference genome mm10 of the UCSC genome (https://genome.ucsc.edu) using STAR software (version 2.5). Cufflinks (version 2.2.1) was used to quantify the mapped reads, and the gene expression values were calculated as fragments per kilobase of transcript per million fragments mapped units.

Differentially expressed genes (DEGs) between CD138^{int} and CD138^{-} FO B cells were analyzed by Cuffdiff software in the Cufflinks package. A cutoff of $p<0.05$ and $|\log_2$ fold change (FC)$| \geq 1$ were considered significant. Volcano plots representing DEGs were generated using the *EnhancedVolcano* package in R with the $\log_{10}$ p-value and $\log_2$ FC (Blighe K, Rana S, Lewis M. Enhanced Volcano: Publication-ready volcano plots with enhanced coloring and labeling. R package version; 1.8.0. https://github.com/kevinblighe/EnhancedVolcano). Gene set enrichment analysis (GSEA; https://www.gsea-msigdb.org) was used to determine whether prior-defined sets of genes showed statistically significant, concordant differences between CD138^{int} and CD138^{-} FO B cells (24).

BCR heavy chain repertoire and data analysis

5×10^6 CD138^{int} and CD138^{-} FO B cells were sorted using pooled splenocytes from five C57BL/6 WT mice and total RNA was amplified for clone-specific rearrangements of the Ig heavy chain genes using the Long Read iR-Reagent System (iRepertoire, Huntsville, AL, USA) at the LAS Laboratory. The quality of the extracted RNA and the generated libraries was evaluated using a 2100 Bioanalyzer RNA Kit with Bioanalyzer RNA Chip and a Bioanalyzer DNA 1000 Chip (Agilent), respectively. 250 bp paired-end sequencing of the pooled libraries was performed on the Illumina MiSeq platform.

For repertoire analysis, raw paired-end fastq files were analyzed using the Immune Repertoire High-throughput Sequence Analysis (IRSA) workflow at the iRepertoire website (https://irweb.irepertoire.com/nir/). Circus plots were obtained using Circos software (http://mkweb.bcgsc.ca) (25). Treemaps representing the diversity and clonality of the repertoires were generated using IRSA. Venn diagram was created using the *Venn diagram* package in R.

To quantify BCR repertoire diversity, Simpson and Shannon indices were calculated for two groups of B cell populations, as described previously (26). A repertoire comparison was performed by calculating Jenson-Shannon divergence (JSD) and Morisita-Horn (MH) similarity indices (27,28). The formulae used for diversity and comparison indices are as follows:

$$\boldsymbol{D} = \sum {p_i}^2$$

$$\boldsymbol{H} = -\sum p_i \log {p_i}^2$$

$$\boldsymbol{JSD}\,(\boldsymbol{P},\boldsymbol{Q}) = \frac{1}{2}\sum p_i \log p_i + \frac{1}{2}\sum q_i \log q_i - \sum\left(\frac{p_i + q_i}{2}\log\left(\frac{p_i + q_i}{2}\right)\right)$$

$$\boldsymbol{C_{MH}}\,(\boldsymbol{P},\boldsymbol{Q}) = \frac{2\sum p_i q_i}{\sum({p_i}^2 + {q_i}^2)}$$

https://doi.org/10.4110/in.2022.22.e50

where D is the Simpson index, H is the Shannon index, JSD (P,Q) is the JSD between populations P and Q, C_{MH} (P,Q) is the MH similarity index between populations P and Q, p_i is the relative abundance of clonotype *i* in a population P, q_i is the relative abundance of clonotype *i* in a population Q, and $p_i + q_i$ is the relative abundance of clonotype *i* in a merged population (P + Q).

Mutation analysis of clonotype sequences was performed using the IMGT database (https://www.imgt.org/; Montpellier, France).

Statistical analysis

Student's t-test (unpaired) and one-way or two-way analysis of variance were used to assess the statistical significance of differences between groups. p-values ≤0.05 was considered statistically significant. Graphs were generated using GraphPad Prism 4.0 (GraphPad Software, San Diego, CA, USA).

RESULTS

CD138^{int} B cells are composed of T3 and FO B cells

First, we investigated at which developmental stage CD138 starts to be expressed after splenic entry of immature B cells from the bone marrow. Overall, CD138^{int} B cells constituted ~11.4% of all splenic B cells (**Fig. 1A**). CD138^{int} B cells were distinguishable from CD138^{high}B220$^{+/-}$ plasma cells and expressed a lower level of IgM and Sca-1 than CD138^{-} B cells, suggesting that CD138^{int} B cells are likely to be anergic B cells with low proliferative potential (29).

Next, we investigated whether the low-level expression of CD138 in B cells was correlated with autoreactivity or the anergic condition, or both. T3 B cells are regarded as anergic B cells that still express the cell surface proteins of immature B cells (17). Then, we checked the proportions of CD138^{int} B cells in subpopulations of transitional and mature B cells in the spleen, which had been gated as shown in **Fig. 1B** and **Supplementary Fig. 1**. The ratios of CD138^{int} B cells were significantly higher in T3 and FO B cells than in other B cell subpopulations (**Fig. 1C**). The average percentages and cell numbers of the CD138^{int} B cells in each population from six mice were expressed as dot plots (**Fig. 1C**, bottom; **Supplementary Fig. 2**). These data suggested that CD138 is expressed at a later stage of splenic B cell maturation and in subpopulations of FO B cells and anergic T3 B cells.

CD138^{int} FO B cells show features of anergic B cells

Since T3 B cells are regarded as anergic B cells, we paid attention to CD138^{int} FO B cells that constituted most of CD138^{int} B cells. To address whether CD138^{int} FO B cells are anergic or chronically activated, the RNA transcriptomes of CD138^{int} and CD138^{-} FO B cells were compared by extracting RNAs from sorted CD138^{int} or CD138^{-} CD23^{+} FO B cells. Differential gene expression was displayed as a volcano plot with relative fold differences and p-values (**Fig. 2A**). Two hundred seventy-seven DEGs with statistical significance ($p \leq 0.05$) were shown with gene names, 114 genes were more highly expressed in CD138^{int} FO B cells, and 163 genes were more highly expressed in CD138^{-} FO B cells. *Pcp4, Iftim1,* and *Hcst* genes were exclusively expressed in CD138^{int} FO B cells, not in CD138^{-} FO B cells. CD138^{int} FO B cells were not biased toward plasma cell differentiation, as they were not enriched in plasma cell surface proteins or transcription factors except *Sdc1* (**Fig. 2B**). CD138^{int} FO B cells also did not upregulate inflammation-related genes. Notably, CD138^{int} FO B cells expressed higher levels of several

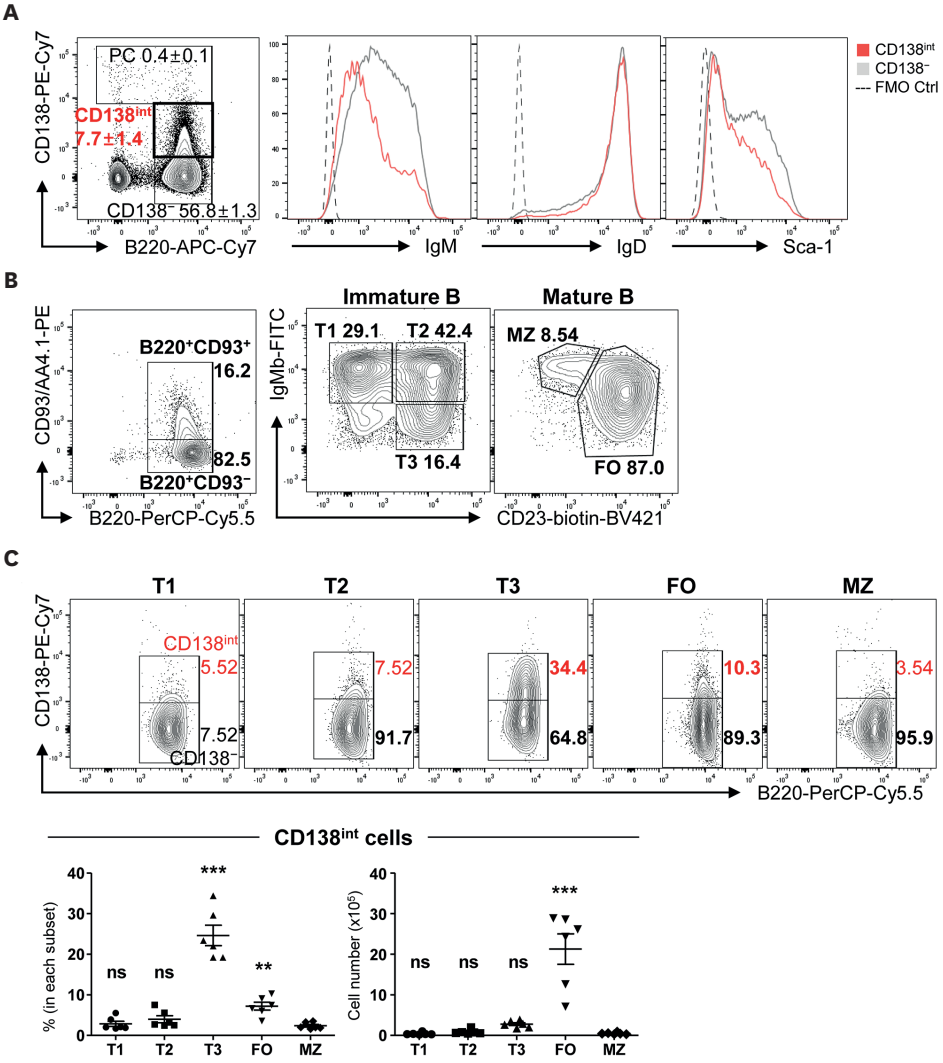

Figure 1. Splenic CD138^{int} B cells belong to FO or T3 B cells in naïve mice. (A) B220 and CD138 expression in live singlet lymphocytes from the spleen of 6- to 8-week-old C57BL/6 WT mice (left). Proportions (±SD) of CD138^{int} and CD138^{-} B cells and CD138^{high} plasma cells (PC). The expression of IgM, IgD, or Sca-1 for gated CD138^{int} (red line) and CD138^{-} (gray line) B cells (right). Fluorescence minus one control (dash line). (B) Splenic cells were stained with Abs against B220, CD93, IgM, CD23, and CD138. Gating strategies for T1, T2, FO, and MZ B cells. (C) CD138 expression in B220^{+} cells for each population (top). Numbers indicate the proportion of CD138^{int} B cells in each population. Average percentages and numbers of CD138^{int} B cells in each population (bottom). Data are representative of six separate experiments. Error bars indicate the SD of individual values, and the statistical significance was determined by Student's t-test.
$^{*}p<0.05$; $^{**}p<0.01$; $^{***}p<0.001$; ns, not significant.

anergy signature genes such as *Pcp4*, *Serp2*, *Tle2*, *Sdc1*, *Rapgef3*, *Ndrg1*, *Rgl1*, *Sox4*, *Myb*, *Fos*, and *Grap2* (**Fig. 2C**, left), which have previously been reported to be high in BCR-transgenic anergic B cells (16,30). The upregulation of *Sdc1* (the gene for CD138) in CD138^{int} FO B cells indicated that the expression of CD138 is transcriptionally regulated. The enrichment of anergy signature genes in CD138^{int} FO B cells was statistically significant in GSEA based on the gene expression in anergic B cells (**Fig. 2C**, middle and right). The GSEA based on genes highly expressed in age-associated B or germinal center B cells suggested that CD138^{int} B cells are neither age-associated B nor germinal center B cells (**Fig. 2D and E**). The high expression of anergic signature genes was further confirmed in CD138^{int} FO B cells compared with CD138^{-} FO B cells by qRT-PCR (**Fig. 2F**).

https://doi.org/10.4110/in.2022.22.e50

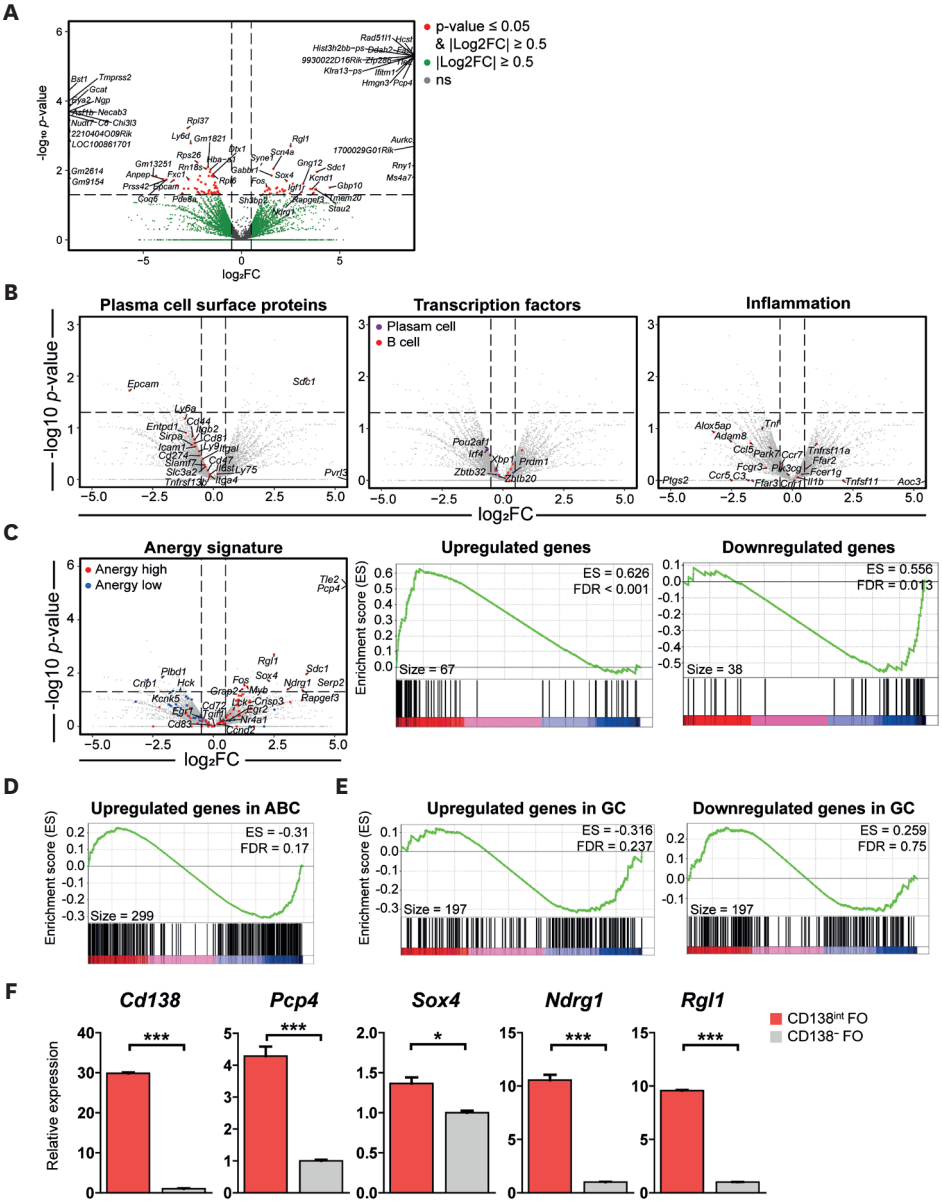

Figure 2. Gene expression comparison between CD138^{int} and CD138^{-} FO B cells. RNA transcriptome analysis was performed using 26,665 genes obtained from sorted CD138^{int} and CD138^{-} CD23^{+}CD21^{-} FO B cells from C57BL/6 WT mice. (A) Volcano plot comparing transcriptomes from CD138^{int} and CD138^{-} FO B cells. Gene symbols for genes with significant differences [p≤0.05 and |$\log_2$ FC| ≥0.5; (red), |$\log_2$ FC| ≤0.5 (green), or no significance (ns, gray)]. (B) Volcano plots comparing transcriptomes from CD138^{int} and CD138^{-} FO B cells with indicated gene clusters: plasma cell surface proteins (53), B cell transcription factors (red) and plasma cell transcription factors (purple) (58), and inflammation (GO:0002675). (C) Volcano plots illustrating upregulated genes (red) or downregulated genes (blue) in anergic B cells (16). Gene set enrichment analysis (GSEA) on a set of 26,665 genes sorted by 67 upregulated genes (left) or 38 downregulated genes (right) in MD4×ML5 anergic B cells (16). (D) GSEA on sets of upregulated genes in ABC versus FO B cells (59). (E) GSEA based on upregulated or downregulated genes in germinal center B cells (GSE11961). (F) qRT-PCR analysis comparing the expressions of *Cd138*, *Pcp4*, *Sox4*, *Ndrg1*, and *Rgl1* in CD138^{int} and CD138^{-} FO B cells. *p<0.05; ***p<0.001; ns, not significant.

The anergic nature of CD138^{int} FO B cells was further confirmed by calcium response and upregulation of CD69 upon BCR engagement. Considering the low expression of IgM in CD138^{int} FO B cells, we stimulated CD138^{int} and CD138^{-} FO B cells with four kinds of Abs for BCR engagement. Anti-IgM and anti-IgD Abs specifically ligated IgM and IgD BCRs, respectively, but anti-IgG and anti-Igκ Abs engaged both IgM and IgD BCRs since they ligated light chains. While CD138^{int} and CD138^{-} FO B cells showed similarly high calcium influx upon

https://doi.org/10.4110/in.2022.22.e50

ionomycin treatment, CD138^{int} FO B cells showed lower calcium influx upon stimulation with 5 or 20 μg/ml anti-IgM than CD138^{-} FO B cells (**Fig. 3A**). The reduction of calcium response in CD138^{int} FO B cells compared to CD138^{-} FO B cells was also seen when cells were stimulated with anti-IgG or anti-Igκ and was not observed when the cells were stimulated with anti-IgD Abs. These results suggest that the calcium response in response to IgM engagement, but not IgD engagement, is different between CD138^{int} and CD138^{-} FO B cells. Interestingly, a reduced calcium response in CD138^{int} FO B cells was observed when cells were stimulated

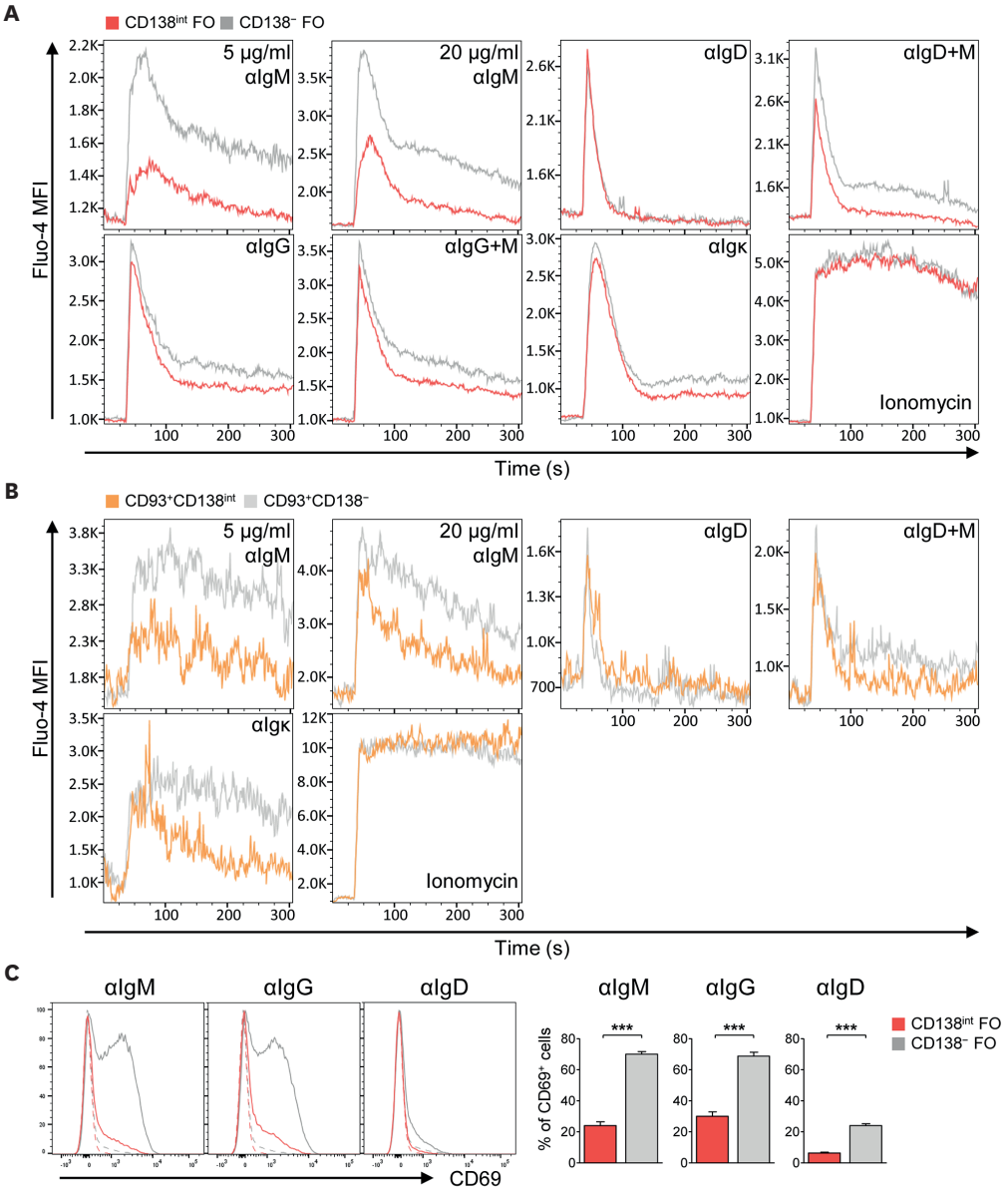

Figure 3. Flow cytometric measurement of B cell cytoplasmic calcium levels using Fluo-4 AM following anti-IgM F(ab')$_2$ or ionomycin treatment. Representative kinetic graphs of average Fluo-4 AM mean fluorescence intensity with time for gated CD138^{int} (red) and CD138^{-} (gray) FO B cells in B220^{+}CD93^{-} cells (A) or gated CD138^{int} (orange) and CD138^{-} (light gray) in B220^{+}CD93^{+} cells (B) in C57BL/6 WT mice. Basal levels were measured for 45 s, and cells were treated with 5 or 20 μg/ml anti-IgM F(ab')$_2$, 20 μg/ml anti-IgG, 1:50 diluted anti-IgD, 20 μg/ml anti-Igκ, or 2 μM ionomycin. (C) Measurement of the CD69 upregulation in CD138^{int} (red) and CD138^{-} (gray) FO B cells that were stimulated with indicated Abs. Splenic B cells were incubated with indicated stimuli for 6 h and the CD69 expression is shown for gated cell populations. Dash lines show the level of unstimulated B cells. Data are representative of three separate experiments. Error bars indicate SD of the mean and the significance was determined by Student's t-test.
***p<0.001.

https://doi.org/10.4110/in.2022.22.e50

with a combination of anti-IgM and anti-IgD Abs, suggesting that the IgM-induced calcium response is reduced by concomitant IgD engagement. The reduction in the calcium response could also be seen in CD138^{int} transitional B cells (**Fig. 3B**). The most significant observation showing the anergic nature of CD138^{int} FO B cells was the failure to upregulate CD69, whereas CD138^{-} FO B cells upregulated the expression of CD69 6 hours after BCR engagement with anti-IgM, anti-IgG, and anti-IgD Abs (**Fig. 3C**). Collectively, CD138^{int} FO B cells exhibited features of anergic B cells based on transcriptional and functional studies.

CD138 expression is regulated by BCR engagement *in vivo*

The CD138 expression was regulated transcriptionally as CD138^{int} FO B cells expressed a higher level of CD138 mRNA than CD138^{-} FO B cells (**Fig. 2A and F**). To investigate whether CD138 expression is regulated by BCR engagement, we estimated the abundance of CD138^{int} B cells in anti-HEL MD4 BCR-transgenic mice. Because most B cells in anti-HEL MD4 transgenic mice are highly specific to HEL and non-autoreactive, anti-HEL B cells did not express CD138 in the homeostatic condition (**Fig. 4A**). However, the percentage of CD138^{int} B cells increased 16–24 h after in vivo injection of HEL in the anti-HEL MD4 transgenic mice, whereas the percentage of CD138^{int} B cells did not increase in the WT mice (**Fig. 4B**). This result suggests that *in vivo* BCR engagement upregulates CD138 expression.

BCR repertoire of CD138^{int} FO B cells is distinct from CD138^{-} FO B cells

Next, BCR heavy chain repertoires were compared between sorted WT CD138^{int} and CD138^{-} FO B cells to explore the BCR repertoire differences between the two populations. The read

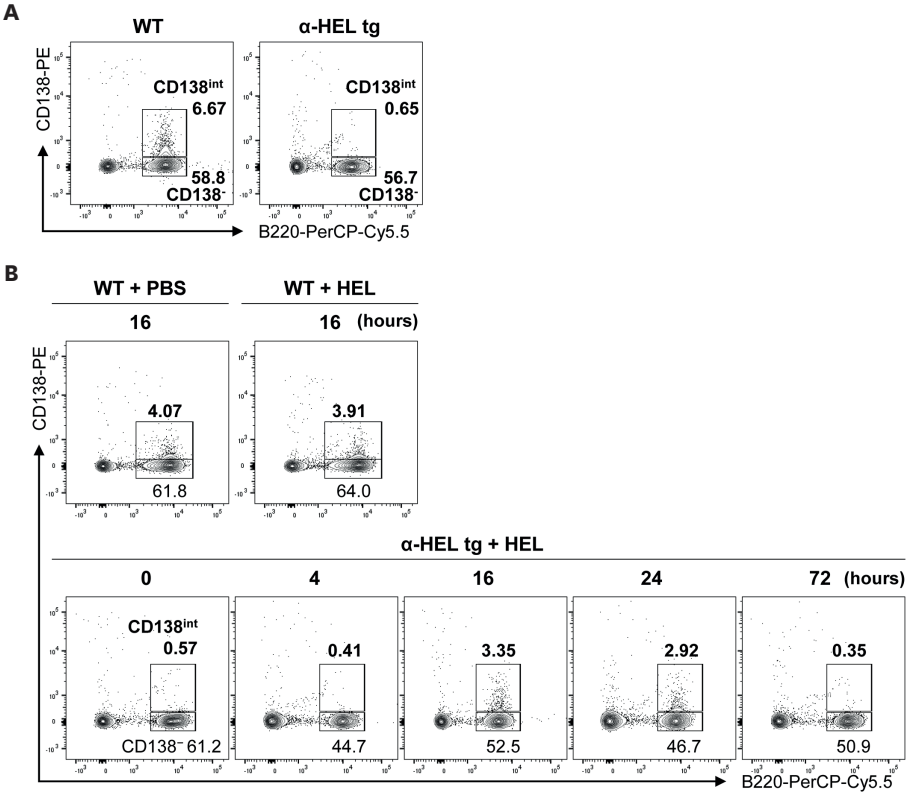

Figure 4. BCR-mediated regulation of the CD138 expression in FO B cells. (A) Splenic cells obtained from C57BL/6 WT and anti-HEL MD4 transgenic mice are shown for the expression of B220 and CD138 by flow cytometric analysis (B). WT and anti-HEL transgenic mice were injected with 100 μg HEL in PBS or PBS only as a control. Splenocytes harvested 4, 16, 24, and 72 h after injection are shown for the expression of B220 and CD138. Data are representative of three separate experiments.

https://doi.org/10.4110/in.2022.22.e50

numbers for analysis are shown in **Supplementary Table 1**. The IgH treemaps of CD138^{int} and CD138^{-} FO B cells showed that both B cell populations were composed of highly diversified IgH CDR3 nucleotide sequences (**Fig. 5A**). Notably, the read numbers of class-switched clonotypes were 56.7% and 28.9% in CD138^{int} and CD138^{-} FO B cells, respectively (**Supplementary Table 1**). However, the proportion of class-switched IgM^{-}IgD^{-} B cells was about 4.75%, suggesting that class-switched mRNA reads were over-represented (**Supplementary Fig. 3**). To compare the repertoires of naïve B cells, we sorted out only Igμ chain sequences and looked for sequences shared between CD138^{int} and CD138^{-} FO B cells. A Venn diagram revealed that only a small fraction of clonotypes was shared between CD138^{int} and CD138^{-} FO B cells and most clonotypes were unique to either CD138^{int} or CD138^{-} FO B cells (**Fig. 5B**). The Igμ chain repertoire of CD138^{-} FO B cells was more diverse than that of CD138^{int} B cells based on Simpson and Shannon indices (**Fig. 5C**). The JSD and MH similarity indices, confirmed the repertoire difference between the

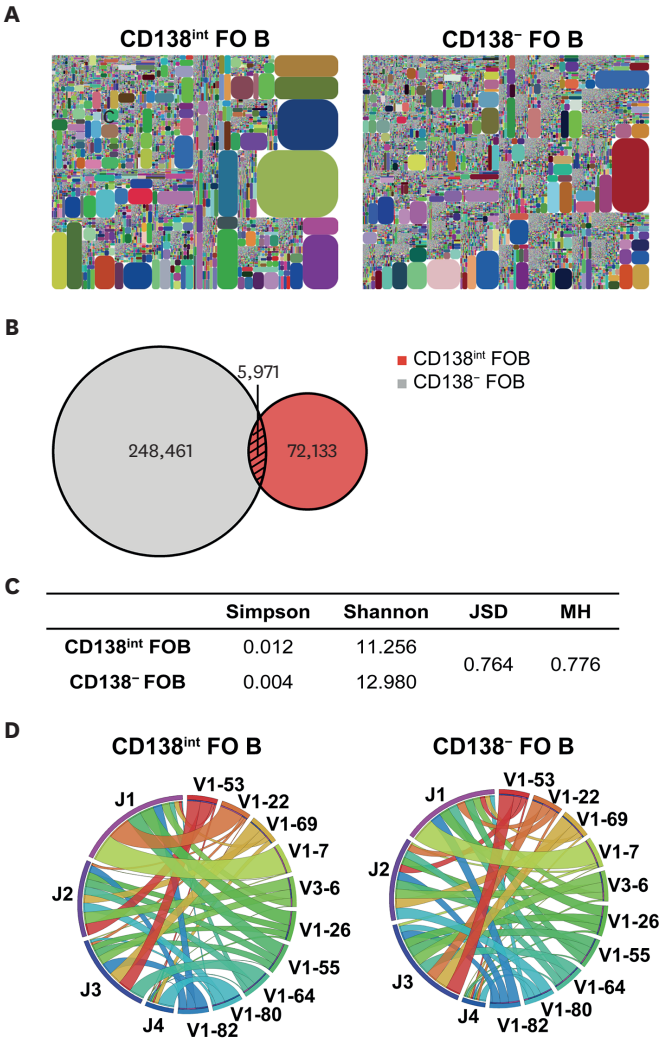

	Simpson	Shannon	JSD	MH
CD138^{int} FOB	0.012	11.256	0.764	0.776
CD138^{-} FOB	0.004	12.980		

Figure 5. BCR heavy chain repertoire analysis of CD138^{int} and CD138^{-} FO B cells. Purified CD138^{int} and CD138^{-} FO B cell subsets from naïve C57BL/6 WT mice were used for Ig heavy chain repertoire analysis. (A) Treemap representation of IgH CDR3 repertoire in CD138^{int} and CD138^{-} FO B cells. (B-D) Clonotypes containing Igμ chain of two repertoires were used for analysis. (B) A Venn diagram showing the number of IgH CDR3 clonotypes in two populations of B cells. The numbers in overlapping areas indicate the number of shared clonotypes between the two. (C) The Simpson and Shannon indices were used to measure the repertoire diversity in CD138^{int} and CD138^{-} FO B cells. The JSD and MH similarity indices were used to calculate the similarity between the two repertoires. (D) Circos plots displaying the V-J linkages for BCR heavy chain repertoires of CD138^{int} and CD138^{-} FO B cells. The top 10 V_H segments were selected and ranked in descending order with respect to the frequencies in the CD138^{int} FO B cell repertoire. The width of the band represents the frequencies of the combined V_H and J_H genes.

https://doi.org/10.4110/in.2022.22.e50

two populations (**Fig. 5C**). When we analyzed the combination between the V_H and J_H segments with Circos plots (**Fig. 5D**), CD138^{int} and CD138$^-$ FO B cells showed discriminating patterns of connections. The frequencies of VH gene usage are shown in **Supplementary Fig. 4**. These results suggest that the two populations were distinctive in the BCR repertoire.

CD138^{int} FO B cells contain more Igμ and class-switched clonotypes with longer CDR3 than CD138$^-$ FO B cells

Next, we compared the WT BCR repertoires of the two B cell populations with respect to class switching, CDR3 length, and rates of somatic mutations. Distribution of IgH subclasses in class-switched clonotypes was shown for CD138^{int} and CD138$^-$ FO B cells (**Fig. 6A**). There was substantial sharing of clonotypes between CD138^{int} IgM clonotypes and CD138^{int} IgD or IgG3 clonotypes as visualized in Venn diagrams (**Fig. 6B**). About one third to one half of all CD138^{int} IgD or IgG3 clonotypes could be found in CD138^{int} IgM clonotypes, respectively. Then, we estimated the repertoire similarities between the clonotypes of given subclasses from CD138^{int} and CD138$^-$ FO B cells (**Fig. 6C**). The JSD values for all combinations were compared to verify whether class-switched CD138^{int} clonotypes developed from CD138^{int} or CD138$^-$ FO B cells. IgG1 and IgG3 class-switched repertoires from CD138^{int} FO cells were more similar to the IgM repertoire from CD138^{int} FO cells than from CD138$^-$ FO B cells, suggesting that class-switched CD138^{int} FO B cells may be derived from unswitched CD138^{int} FO B cells rather than unswitched CD138$^-$ FO B cells. Furthermore, all subclasses of CD138^{int} B cells had a higher proportion of long CDR3 sequences than those of CD138$^-$ B cells (**Fig. 6D**). However, the rates of somatic mutations were low and comparable between the two B cell populations except for IgG1 (**Fig. 6E**). These results suggest that CD138^{int} B cells may be autoreactive B cells, as BCRs with long CDR3 sequences tend to be autoreactive (2,31). Class-switched CD138^{int} B cells appeared to be derived from extrafollicular B cell responses of unswitched CD138^{int} B cells since they do not accumulate high levels of somatic mutations.

DISCUSSION

CD138 is a type I transmembrane protein glycosylated with chondroitin and heparan sulfate moieties. Heparan sulfate moieties bind pro-survival cytokines that provide a survival advantage for plasma cells (32,33). Although the high level expression of CD138 is used to identify plasma cells, the significance of a low-level expression of CD138 is not yet understood. Its low-level expression is also observed on bone marrow precursor B cells and subpopulations of FO B cells (22). This study shows that splenic CD138^{int} B cells are anergic FO or T3 B cells, but not plasma cells or germinal center B cells. This observation suggests that the CD138^{int} B cells may be under chronic stimulation through autoreactive BCRs. Since the expression of CD138 increases spontaneously in *in vitro* culture of FO B cells (22), it is difficult to show the upregulation of CD138 upon BCR engagement in *in vitro* experiments. Previously, the low-level expression of CD138 has been shown when anti-HEL B cells were forced to constitutively encounter HEL Ag in MD5 × ML5 double transgenic mice (34). In the current study, we showed the upregulation of CD138 in anti-HEL B cells 16 hours after *in vivo* injection of HEL. We hypothesize that the expression of CD138 is delicately regulated *in vivo* and is upregulated by chronic stimulation via BCR in a similar manner to NOD1 or Nur77 (35,36).

Naïve FO B cells express both IgM and IgD BCRs, but these two isotypes of BCR are segregated into distinct clusters in the plasma membrane and have different functions (37). Anergic autoreactive B cells have been shown to have high levels of IgD BCR, which is less

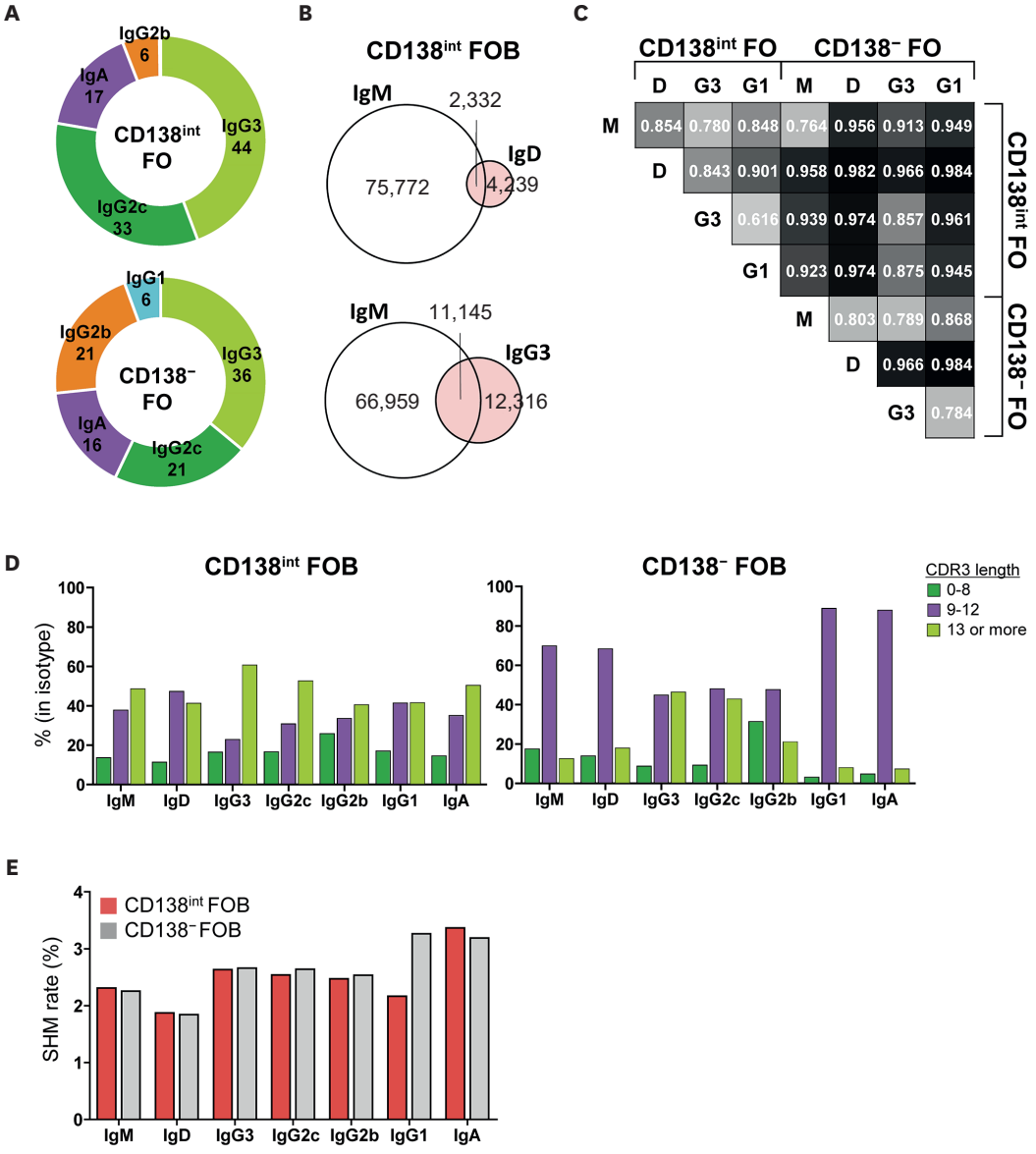

Figure 6. Comparison of Ig heavy chain isotype frequencies, CDR3 lengths, and somatic mutations between CD138^{int} and CD138^{-} FO B cells. (A) Pie charts illustrating the percentages of clonotypes with given class switching among all class-switched clonotypes in the BCR repertoires of CD138^{int} and CD138^{-} FO B cell subsets from naïve C57BL/6 WT mice. (B) Venn diagrams showing the numbers of common and distinct clonotypes of IgM and IgD or IgG3 in the CD138^{int} FO B cell repertoire. (C) Heatmap showing JSD values comparing IgH repertoires of individual isotypes from the two populations. When JSD = 1, two populations are completely distinct. Smaller JSD values indicate more similarity between the two populations under comparison. (D) The CDR3 length (number of amino acid residues) distribution in the indicated isotypes of CD138^{int} and CD138^{-} FO B cells. (E) Average somatic mutation rates (mutated nucleotide/total nucleotides) in all clonotypes belonging to the indicated isotypes of CD138^{int} or CD138^{-} FO B cells.

sensitive to endogenous Ags than IgM BCR (38,39). When naïve IgM^{+}IgD^{+} B cells encounter specific Ags, IgM BCRs respond quickly to the Ags and undergo selective endocytosis, in contrast to IgD BCRs (40). Because autoreactive IgM^{+}IgD^{+} B cells meet endogenous Ags in homeostatic conditions, the selective downregulation of IgM BCR generates IgM^{low}IgD^{high} B cells. However, the expression levels of IgM and IgD cannot discriminate highly autoreactive FO B cells from less autoreactive FO B cells because most FO B cells show the IgM^{low}IgD^{high} phenotype with continuous levels of variability of the two isotypes of BCRs. As reported previously, FO B cells are selected based on a modest level of autoreactivity (41). Furthermore, the expression of Nur77 in most FO B cells demonstrates that most FO B cells encounter Ag

https://doi.org/10.4110/in.2022.22.e50

during development (13). Interestingly, the BCR signaling experience does not lead to B-cell anergy if BCR affinity to Ag is low or the Ag amount is low (5). Therefore, autoreactive FO B cells can be immunocompetent or anergic depending on the strength and quality of BCR-mediated signaling and the abundance of autoantigens.

BCR-mediated signaling is essential for B cell development and functions. BCRs induce different signals at various stages and upon binding to Ags with low or high affinities. First, BCRs can signal independently of ligand engagement and induce tonic signaling for B cell survival (42). This survival signaling is triggered via immunoreceptor tyrosine-based activation motifs of Igα and Igβ and phosphatidylinositol 3-kinases (43,44). This weak tonic signaling is a checkpoint signal for B cell development and maturation. B cells with moderate to high affinity to self-Ags further trigger canonical nuclear factor-κB signaling and the consequent production of p100 transcription, which can be processed by BAFF-R signaling upon binding to BAFF (41). Therefore, the survival of FO B cells requires a high level of BCR-mediated signaling, and moderately autoreactive B cells are selected as FO B cells. This moderate BCR signaling may lead to Nur77 expression in most FO B cells (13). Highly autoreactive B cells require a much higher level of BAFF for their survival (45). Interestingly, PCP4 expression could be an indicator of high autoreactivity as PCP4 was highly expressed in the CD138^{int} FO B cells. Both Nur77 and PCP4 have been reported as negative signaling regulators to suppress excessive activation (46,47). Collectively, autoreactive B cells are not always deleted but can survive under certain conditions of signaling networks. Furthermore, moderate autoreactivity and cross-reactivity to foreign Ags prime individual cells for optimal proliferative responses following Ag exposure (48).

The negative selection of autoreactive B cells was first demonstrated in experiments using transgenic mice expressing both engineered Ag and BCRs specific to the Ag (49,50). The affinity constants of the interaction between the transgenic Ags and BCRs are typically very high, as BCRs are derived from highly specific B cells of mice previously immunized with model Ags, such as HEL, and K_a for anti-HEL for HEL is ~10^{10} M^{-1} (51). The negative selection of transgenic B cells in the presence of Ag has been shown to be dramatic, but notably, the elimination of autoreactive B cells was not complete, resulting in the persistence of a substantial number of autoreactive B cells as anergic B cells in the mature B cell repertoire (2,13). Elimination of autoreactive B cells is executed during multiple stages of B cell development through several different mechanisms such as clonal deletion, BCR editing, anergy induction, and FO exclusion (52). A pitfall of the experiments with the transgenic BCRs is the very high affinity of transgenic BCRs to the engineered Ags, which is unusual with germline BCRs in the actual naïve B cells. Therefore, the study of negative selection using transgenic B cells does not reflect the destiny of germline autoreactive B cells with moderate autoreactivity.

It can be debated whether CD138^{int} B cells are pre-plasma cells. Although CD138^{high} plasma cells are irreversibly committed cells, CD138^{int} B cells are not committed cells and CD138 expression can be reversed by cytokines such as IL-4 (22). CD138^{int} B cells may be in a tolerance checkpoint before plasma cell differentiation to prevent the production of autoreactive Abs as previously described (34). Expansion of CD138^{int} B cells has been noted in autoimmune disease models, and these B cells were mentioned as pre-plasma cells (34). The frequency of intracytoplasmic IgM^{+} antibody-secreting cells has been found to be higher in CD138^{int} B cells than in CD138^{-} B cells, but the percentage of antibody-secreting cells in CD138^{int} B cells was found to be less than 5% (34). Therefore, most CD138^{int} FO B cells are not committed to plasma cells but maintain their B cell identity. Cell surface proteins in plasma cells were recently elucidated by investigating Blimp-1-expressing cells (53). Our data showed that

CD138^{int} B cells did not express any of the plasma cell surface proteins mentioned in the article, except CD138. Therefore, CD138^{int} B cells were thought to be chronically activated autoreactive B cells and suppressed not to differentiate into plasma cells. We hypothesize that variable numbers of autoreactive CD138^{int} B cells accumulate as a checkpoint stage in the normal or autoimmune-prone mice and some CD138^{int} B cells eventually escape the regulation mechanism and become plasma cells in autoimmune disease models, such as MLR/*lpr* mice.

Autoreactive B cells are not thought to be always harmful to the host. They may provide beneficial autoantibodies that contribute to the clearance of altered or damaged self-Ags and prevent the appearance of high-affinity Abs to self (1). It was surprising to observe that ~5% of CD138^{int} FO B cells were class-switched mainly to IgG3, IgG2c, and IgA. IgG3, IgG2c, and IgA heavy chain sequences were significantly enriched in CD138^{int} FO B cells compared to CD138^{-} FO B cells. However, class-switched Ig heavy chain sequences from CD138^{int} FO B cells did not show more somatic hypermutations than those from CD138^{-} FO B cells. This finding may suggest that class-switched CD138^{int} FO B cells are not derived from the germinal center reaction but from the T cell-independent pathway. Natural IgG or IgA autoantibodies have been described in humans and mice, contributing to innate protection against pathogens and the removal of altered self-materials (54-56). The contribution of CD138^{int} FO B cells to the production of natural IgG or IgA autoantibodies requires further investigation.

Anergy is a state of long-term hyporesponsiveness of lymphocytes, clearly defined in T cells (57). The anergic state is maintained by chronic antigenic stimulation. Although anergic B cells appear to be relatively abundant based on the Nur77 expression in most FO B cells (13), it has been difficult to identify anergic B cells except T3 transitional B cells based on cell surface markers. Previously, anergic B cells have been defined on a genetic basis so that anti-HEL B cells are regarded as anergic B cells in the background of HEL expression. This study describes polyclonal anergic CD138^{int} FO and T3 B cells in WT mice. We hypothesize a model of anergic B cells that are heterogeneous and include T3 and CD138^{int} FO B cells (**Fig. 7**). We currently do not

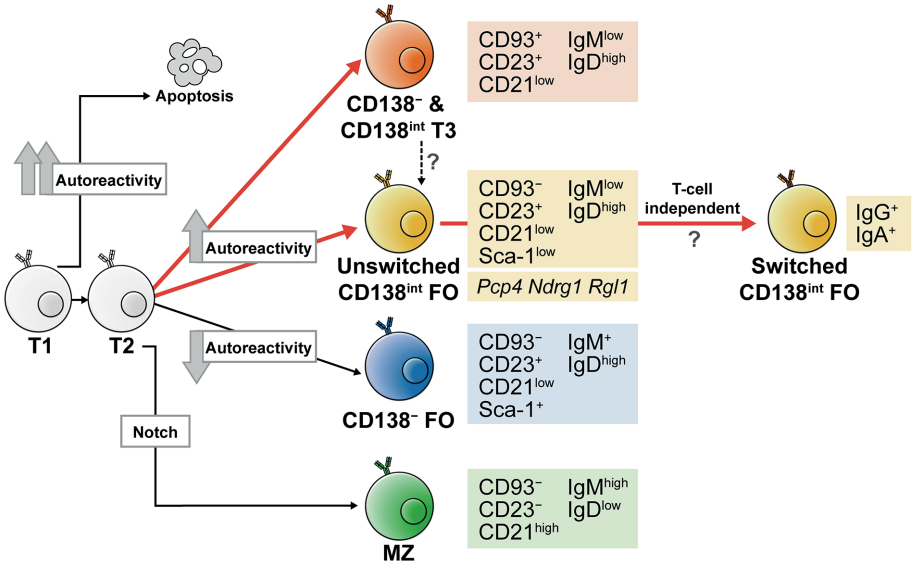

Figure 7. Schematic diagram representing the development of CD138^{int} B cells. Transitional B cells undergo different fates based on BCR autoreactivity. Strongly autoreactive B cells are deleted or excluded from the follicular entrance, but a substantial proportion of autoreactive B cells remain as anergic T3 or FO B cells. Anergic FO B cells are identified as CD138^{int}CD23^{+}CD21^{-} B cells and express listed genes. Anergic FO B cells may undergo class switching with low-level somatic mutations, which is common in T cell-independent antibody responses.

https://doi.org/10.4110/in.2022.22.e50

understand why some anergic B cells become mature FO B cells and undergo class switching, not remaining as transitional B cells. It needs to address whether they contribute to the pathogenesis of autoimmune diseases or the production of natural Abs in the homeostatic condition.

ACKNOWLEDGEMENTS

This research was supported by the Korea Medical Device Development Fund (grants KMDF_PR_20200901_0004 and NTIS 9991006677) from the Korean Government (the Ministry of Science and ICT, the Ministry of Trade, Industry and Energy, the Ministry of Health and Welfare, and the Ministry of Food and Drug Safety), the Korea Basic Science Institute (National Research Facilities and Equipment Center) grant (2020R1A6C101A191) of the Ministry of Education (Korea) and National Research Foundation of Korea, and the BK21 FOUR Program (Graduate School Innovation) of Sungkyunkwan University.

SUPPLEMENTARY MATERIALS

Supplementary Table 1

Numbers of Ig reads in indicated isotypes from CD138^{int} and CD138^{-} FO B cells

Click here to view

Supplementary Figure 1

Gating strategy for CD138^{high}, CD138^{int}, and CD138^{-} B cells. (a) 7AAD^{-} live singlet cells in the lymphocyte gating are shown for the expression of B220 and CD138. (b) CD19^{+} or B220^{+} B cells gated from 7AAD^{-} live singlet cells in the lymphocyte gating are further shown for the expression of B220 and CD138. (c) B220^{+}CD93^{+} transitional B cells are further gated from CD19^{+} or B220^{+} B cells and shown for the expression of B220 and CD138.

Click here to view

Supplementary Figure 2

CD138^{int} B cells in marginal zone B precursor (MZP). (A) Splenic cells were stained with anti-B220, CD21, CD24, CD93, CD23, and CD138 antibodies. Gating strategy based on Srivastava et al (60). Numbers indicate the percentages (±SD) of CD138^{int} B cells in each subset. (B) The proportion (left) or absolute cell number (right) of CD138^{int} B cells.

Click here to view

Supplementary Figure 3

IgM^{-}IgD^{-} CD138^{int} B cells. Splenocytes were stained with anti-CD19, IgDb, IgM, CD138, and B220 antibodies. Class-switched isotypes were evaluated CD19^{+}IgD^{-}IgM^{-} B cells. Most CD138^{int} B cells expressed IgD^{+}IgM^{-} but few CD138^{int} B cells expressed class-switched Ig.

Click here to view

IMMUNE NETWORK

Supplementary Figure 4

V_H segment usage in Ig isotypes from $CD138^{int}$ and $CD138^-$ FO B cells. V_H segment usage listed in descending order with respect to the frequency of $CD138^{int}$ FO B cells on top 30 in indicated isotypes.

Click here to view

REFERENCES

1. Lee S, Ko Y, Kim TJ. Homeostasis and regulation of autoreactive B cells. *Cell Mol Immunol* 2020;17:561-569.
PUBMED | CROSSREF
2. Wardemann H, Yurasov S, Schaefer A, Young JW, Meffre E, Nussenzweig MC. Predominant autoantibody production by early human B cell precursors. *Science* 2003;301:1374-1377.
PUBMED | CROSSREF
3. Liu Z, Davidson A. BAFF and selection of autoreactive B cells. *Trends Immunol* 2011;32:388-394.
PUBMED | CROSSREF
4. Shlomchik MJ. Sites and stages of autoreactive B cell activation and regulation. *Immunity* 2008;28:18-28.
PUBMED | CROSSREF
5. Gaudin E, Hao Y, Rosado MM, Chaby R, Girard R, Freitas AA. Positive selection of B cells expressing low densities of self-reactive BCRs. *J Exp Med* 2004;199:843-853.
PUBMED | CROSSREF
6. Nemazee D. Mechanisms of central tolerance for B cells. *Nat Rev Immunol* 2017;17:281-294.
PUBMED | CROSSREF
7. Meffre E, Wardemann H. B-cell tolerance checkpoints in health and autoimmunity. *Curr Opin Immunol* 2008;20:632-638.
PUBMED | CROSSREF
8. Grimaldi CM, Hicks R, Diamond B. B cell selection and susceptibility to autoimmunity. *J Immunol* 2005;174:1775-1781.
PUBMED | CROSSREF
9. Pelanda R, Torres RM. Central B-cell tolerance: where selection begins. *Cold Spring Harb Perspect Biol* 2012;4:a007146.
PUBMED | CROSSREF
10. Schmidt KN, Cyster JG. Follicular exclusion and rapid elimination of hen egg lysozyme autoantigen-binding B cells are dependent on competitor B cells, but not on T cells. *J Immunol* 1999;162:284-291.
PUBMED
11. Turner M, Gulbranson-Judge A, Quinn ME, Walters AE, MacLennan IC, Tybulewicz VL. Syk tyrosine kinase is required for the positive selection of immature B cells into the recirculating B cell pool. *J Exp Med* 1997;186:2013-2021.
PUBMED | CROSSREF
12. Tan C, Noviski M, Huizar J, Zikherman J. Self-reactivity on a spectrum: a sliding scale of peripheral B cell tolerance. *Immunol Rev* 2019;292:37-60.
PUBMED | CROSSREF
13. Zikherman J, Parameswaran R, Weiss A. Endogenous antigen tunes the responsiveness of naive B cells but not T cells. *Nature* 2012;489:160-164.
PUBMED | CROSSREF
14. Goodnow CC, Crosbie J, Adelstein S, Lavoie TB, Smith-Gill SJ, Brink RA, Pritchard-Briscoe H, Wotherspoon JS, Loblay RH, Raphael K, et al. Altered immunoglobulin expression and functional silencing of self-reactive B lymphocytes in transgenic mice. *Nature* 1988;334:676-682.
PUBMED | CROSSREF
15. Gauld SB, Benschop RJ, Merrell KT, Cambier JC. Maintenance of B cell anergy requires constant antigen receptor occupancy and signaling. *Nat Immunol* 2005;6:1160-1167.
PUBMED | CROSSREF
16. Sabouri Z, Perotti S, Spierings E, Humburg P, Yabas M, Bergmann H, Horikawa K, Roots C, Lambe S, Young C, et al. IgD attenuates the IgM-induced anergy response in transitional and mature B cells. *Nat Commun* 2016;7:13381.
PUBMED | CROSSREF

17. Merrell KT, Benschop RJ, Gauld SB, Aviszus K, Decote-Ricardo D, Wysocki LJ, Cambier JC. Identification of anergic B cells within a wild-type repertoire. *Immunity* 2006;25:953-962.
PUBMED | CROSSREF
18. Duty JA, Szodoray P, Zheng NY, Koelsch KA, Zhang Q, Swiatkowski M, Mathias M, Garman L, Helms C, Nakken B, et al. Functional anergy in a subpopulation of naive B cells from healthy humans that express autoreactive immunoglobulin receptors. *J Exp Med* 2009;206:139-151.
PUBMED | CROSSREF
19. Chernova I, Jones DD, Wilmore JR, Bortnick A, Yucel M, Hershberg U, Allman D. Lasting antibody responses are mediated by a combination of newly formed and established bone marrow plasma cells drawn from clonally distinct precursors. *J Immunol* 2014;193:4971-4979.
PUBMED | CROSSREF
20. Wilmore JR, Jones DD, Allman D. Protocol for improved resolution of plasma cell subpopulations by flow cytometry. *Eur J Immunol* 2017;47:1386-1388.
PUBMED | CROSSREF
21. Boldison J, Da Rosa LC, Buckingham L, Davies J, Wen L, Wong FS. Phenotypically distinct anti-insulin B cells repopulate pancreatic islets after anti-CD20 treatment in NOD mice. *Diabetologia* 2019;62:2052-2065.
PUBMED | CROSSREF
22. Lee JG, Moon H, Park C, Shin SH, Kang K, Kim TJ. Reversible expression of CD138 on mature follicular B cells is downregulated by IL-4. *Immunol Lett* 2013;156:38-45.
PUBMED | CROSSREF
23. Mason DY, Jones M, Goodnow CC. Development and follicular localization of tolerant B lymphocytes in lysozyme/anti-lysozyme IgM/IgD transgenic mice. *Int Immunol* 1992;4:163-175.
PUBMED | CROSSREF
24. Subramanian A, Tamayo P, Mootha VK, Mukherjee S, Ebert BL, Gillette MA, Paulovich A, Pomeroy SL, Golub TR, Lander ES, et al. Gene set enrichment analysis: a knowledge-based approach for interpreting genome-wide expression profiles. *Proc Natl Acad Sci U S A* 2005;102:15545-15550.
PUBMED | CROSSREF
25. Briney BS, Willis JR, McKinney BA, Crowe JE Jr. High-throughput antibody sequencing reveals genetic evidence of global regulation of the naïve and memory repertoires that extends across individuals. *Genes Immun* 2012;13:469-473.
PUBMED | CROSSREF
26. Chaudhary N, Wesemann DR. Analyzing immunoglobulin repertoires. *Front Immunol* 2018;9:462.
PUBMED | CROSSREF
27. DeWolf S, Grinshpun B, Savage T, Lau SP, Obradovic A, Shonts B, Yang S, Morris H, Zuber J, Winchester R. Quantifying size and diversity of the human T cell alloresponse. *JCI Insight* 2018;3:e121256.
PUBMED | CROSSREF
28. Venturi V, Kedzierska K, Tanaka MM, Turner SJ, Doherty PC, Davenport MP. Method for assessing the similarity between subsets of the T cell receptor repertoire. *J Immunol Methods* 2008;329:67-80.
PUBMED | CROSSREF
29. Fossati V, Kumar R, Snoeck HW. Progenitor cell origin plays a role in fate choices of mature B cells. *J Immunol* 2010;184:12511260.
PUBMED | CROSSREF
30. Glynne R, Ghandour G, Rayner J, Mack DH, Goodnow CC. B-lymphocyte quiescence, tolerance and activation as viewed by global gene expression profiling on microarrays. *Immunol Rev* 2000;176:216-246.
PUBMED | CROSSREF
31. Klonowski KD, Primiano LL, Monestier M. Atypical VH-D-JH rearrangements in newborn autoimmune MRL mice. *J Immunol* 1999;162:1566-1572.
PUBMED
32. Wijdenes J, Dore JM, Clement C, Vermot-Desroches C. CD138. *J Biol Regul Homeost Agents* 2002;16:152-155.
PUBMED
33. Moreaux J, Sprynski AC, Dillon SR, Mahtouk K, Jourdan M, Ythier A, Moine P, Robert N, Jourdan E, Rossi JF, et al. APRIL and TACI interact with syndecan-1 on the surface of multiple myeloma cells to form an essential survival loop. *Eur J Haematol* 2009;83:119-129.
PUBMED | CROSSREF
34. Culton DA, O'Conner BP, Conway KL, Diz R, Rutan J, Vilen BJ, Clarke SH. Early preplasma cells define a tolerance checkpoint for autoreactive B cells. *J Immunol* 2006;176:790-802.
PUBMED | CROSSREF
35. Huizar J, Tan C, Noviski M, Mueller JL, Zikherman J. Nur77 is upregulated in B-1a cells by chronic self-antigen stimulation and limits generation of natural IgM plasma cells. *Immunohorizons* 2017;1:188-197.
PUBMED | CROSSREF

36. Hayakawa K, Formica AM, Zhou Y, Ichikawa D, Asano M, Li YS, Shinton SA, Brill-Dashoff J, Núñez G, Hardy RR. NLR Nod1 signaling promotes survival of BCR-engaged mature B cells through up-regulated Nod1 as a positive outcome. *J Exp Med* 2017;214:3067-3083.
PUBMED | CROSSREF

37. Hobeika E, Maity PC, Jumaa H. Control of B cell responsiveness by isotype and structural elements of the antigen receptor. *Trends Immunol* 2016;37:310-320.
PUBMED | CROSSREF

38. Übelhart R, Hug E, Bach MP, Wossning T, Dühren-von Minden M, Horn AH, Tsiantoulas D, Kometani K, Kurosaki T, Binder CJ, et al. Responsiveness of B cells is regulated by the hinge region of IgD. *Nat Immunol* 2015;16:534-543.
PUBMED | CROSSREF

39. Noviski M, Zikherman J. Control of autoreactive B cells by IgM and IgD B cell receptors: maintaining a fine balance. *Curr Opin Immunol* 2018;55:67-74.
PUBMED | CROSSREF

40. Noviski M, Mueller JL, Satterthwaite A, Garrett-Sinha LA, Brombacher F, Zikherman J. IgM and IgD B cell receptors differentially respond to endogenous antigens and control B cell fate. *eLife* 2018;7:e35074.
PUBMED | CROSSREF

41. Cancro MP. Signalling crosstalk in B cells: managing worth and need. *Nat Rev Immunol* 2009;9:657-661.
PUBMED | CROSSREF

42. Monroe JG. ITAM-mediated tonic signalling through pre-BCR and BCR complexes. *Nat Rev Immunol* 2006;6:283-294.
PUBMED | CROSSREF

43. Okkenhaug K. Signaling by the phosphoinositide 3-kinase family in immune cells. *Annu Rev Immunol* 2013;31:675-704.
PUBMED | CROSSREF

44. Srinivasan L, Sasaki Y, Calado DP, Zhang B, Paik JH, DePinho RA, Kutok JL, Kearney JF, Otipoby KL, Rajewsky K. PI3 kinase signals BCR-dependent mature B cell survival. *Cell* 2009;139:573-586.
PUBMED | CROSSREF

45. Batten M, Groom J, Cachero TG, Qian F, Schneider P, Tschopp J, Browning JL, Mackay F. BAFF mediates survival of peripheral immature B lymphocytes. *J Exp Med* 2000;192:1453-1466.
PUBMED | CROSSREF

46. Tan C, Hiwa R, Mueller JL, Vykunta V, Hibiya K, Noviski M, Huizar J, Brooks JF, Garcia J, Heyn C, et al. NR4A nuclear receptors restrain B cell responses to antigen when second signals are absent or limiting. *Nat Immunol* 2020;21:1267-1279.
PUBMED | CROSSREF

47. Kim EE, Shekhar A, Lu J, Lin X, Liu FY, Zhang J, Delmar M, Fishman GI. PCP4 regulates Purkinje cell excitability and cardiac rhythmicity. *J Clin Invest* 2014;124:5027-5036.
PUBMED | CROSSREF

48. Steach HR, DeBuysscher BL, Schwartz A, Boonyaratanakornkit J, Baker ML, Tooley MR, Pease NA, Taylor JJ. Cross-reactivity with self-antigen tunes the functional potential of naive B cells specific for foreign antigens. *J Immunol* 2020;204:498-509.
PUBMED | CROSSREF

49. Melamed D, Benschop RJ, Cambier JC, Nemazee D. Developmental regulation of B lymphocyte immune tolerance compartmentalizes clonal selection from receptor selection. *Cell* 1998;92:173-182.
PUBMED | CROSSREF

50. Mandik-Nayak L, Bui A, Noorchashm H, Eaton A, Erikson J. Regulation of anti-double-stranded DNA B cells in nonautoimmune mice: localization to the T-B interface of the splenic follicle. *J Exp Med* 1997;186:1257-1267.
PUBMED | CROSSREF

51. Cyster JG, Healy JI, Kishihara K, Mak TW, Thomas ML, Goodnow CC. Regulation of B-lymphocyte negative and positive selection by tyrosine phosphatase CD45. *Nature* 1996;381:325-328.
PUBMED | CROSSREF

52. Basten A, Silveira PA. B-cell tolerance: mechanisms and implications. *Curr Opin Immunol* 2010;22:566-574.
PUBMED | CROSSREF

53. Dang VD, Mohr E, Szelinski F, Le TA, Ritter J, Hinnenthal T, Stefanski AL, Schrezenmeier E, Ocvirk S, Hipfl C, et al. CD39 and CD326 are bona fide markers of murine and human plasma cells and identify a bone marrow specific plasma cell subpopulation in lupus. *Front Immunol* 2022;13:873217.
PUBMED | CROSSREF

54. Panda S, Ding JL. Natural antibodies bridge innate and adaptive immunity. *J Immunol* 2015;194:13-20.
PUBMED | CROSSREF

55. Panda S, Zhang J, Tan NS, Ho B, Ding JL. Natural IgG antibodies provide innate protection against ficolin-opsonized bacteria. *EMBO J* 2013;32:2905-2919.
PUBMED | CROSSREF

56. Aung KM, Sjöström AE, von Pawel-Rammingen U, Riesbeck K, Uhlin BE, Wai SN. Naturally occurring IgG antibodies provide innate protection against vibrio cholerae bacteremia by recognition of the outer membrane protein U. *J Innate Immun* 2016;8:269-283.
PUBMED | CROSSREF

57. Chappert P, Schwartz RH. Induction of T cell anergy: integration of environmental cues and infectious tolerance. *Curr Opin Immunol* 2010;22:552-559.
PUBMED | CROSSREF

58. Kassambara A, Rème T, Jourdan M, Fest T, Hose D, Tarte K, Klein B. GenomicScape: an easy-to-use web tool for gene expression data analysis. Application to investigate the molecular events in the differentiation of B cells into plasma cells. *PLOS Comput Biol* 2015;11:e1004077.
PUBMED | CROSSREF

59. Masle-Farquhar E, Peters TJ, Miosge LA, Parish IA, Weigel C, Oakes CC, Reed JH, Goodnow CC. Uncontrolled CD21^{low} age-associated and B1 B cell accumulation caused by failure of an EGR2/3 tolerance checkpoint. *Cell Reports* 2022;38:110259.
PUBMED | CROSSREF

60. Srivastava B, Quinn WJ 3rd, Hazard K, Erikson J, Allman D. Characterization of marginal zone B cell precursors. *J Exp Med* 2005;202:1225-1234.
PUBMED | CROSSREF